ELSEVIER

Ceramics International 30 (2004) 683–687

CERAMICS INTERNATIONAL

www.elsevier.com/locate/ceramint

A functional gradient ceramic monomorph actuator fabricated using electrophoretic deposition

Y.H. Chen*, J. Ma, T. Li

School of Materials Engineering, Nanyang Technological University, Nanyang Avenue, 639798, Singapore

Received 27 March 2003; received in revised form 7 July 2003; accepted 10 August 2003

Available online 17 March 2004

Abstract

The fabrication process of FGM monomorph actuator fabricated by the EPD technique is described in detail as well as its graded microstructure. The principle of the monomorph is discussed and the expression for the theoretical bending displacement is derived. Good agreement is observed between the theoretical predictions and the experimental results.

Keywords: FGM; Monomorph; EPD; Displacement

1. Introduction

Piezoelectric ceramics such as lead zirconate-titanate (PZT) are widely used in applications such as actuators, transducers, and micropositioners [1]. Piezoelectric bimorph is a typical piezoelectric device that can produce relatively large displacement [2]. In general, it consists of two piezoelectric ceramic plates bonded together. Application of an external electric field across the piezoelectric plates can then result in a transverse deflection due to the axial contraction of one plate and extension of the other plate. However, severe disadvantages such as low reliability and poor interfacial bonding conditions have been limiting the use of the bimorph. It is therefore desirable to develop a monomorph with minimized internal stress peaks when voltage is applied and also with minimum structural dissimilarities that can cause failure with cyclic strains.

Recently, the concept of "Functionally Gradient" has been proposed for such monomorph [3–6]. In this paper, an improved FGM monomorph is introduced and characterized. The component has a functionally gradient composition over the cross section. This structure is found to optimize the stress distribution and hence increase the reliability of the component.

The current FGM monomorph is fabricated using electrophoretic deposition (EPD) technique, which is a promising and useful preparation method for functionally gradient and multilayer composites. The advantages of the EPD technique are [7–9]: (1) the process is simple and low cost, (2) it is possible to deposit various oxides on conductive substrates which have detailed and complex shapes and (3) it is a flexible method for the production of both thin and thick coatings.

In this paper, the aims are to introduce the fabrication process of the monomorph using EPD technique; establish the constitutive relationships between the bending displacement and related parameters; and finally conduct experimental verification.

2. Theoretical displacement

To derive the theoretical bending displacement of the FGM monomorph actuator, its structure is assumed to consist of n equal layers with functional gradient over the cross section. The dimension of this actuator is l in length, w in width and h in thickness. As shown in Fig. 1, the origin of the coordinate system is positioned at the bottom surface of the actuator. The x-, y- and z-axis are along the length, width and thickness direction, respectively.

In the present work, we adopt the conventional approximation [10], i.e., (1) the total thickness and the width w are

* Corresponding author. Tel.: +65-67904590; fax: +65-67900920.
E-mail address: PG01185880@ntu.edu.sg (Y.H. Chen).

0272-8842/$30.00
doi:10.1016/j.ceramint.2003.08.008

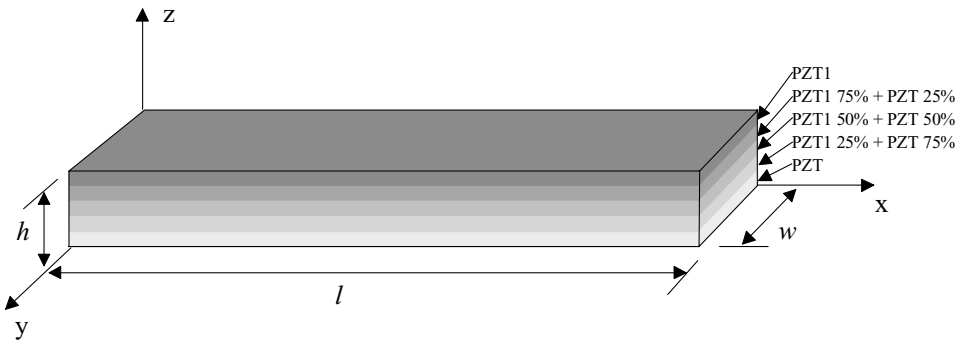

Fig. 1. Structure and composition profile of PZT–PZT1 FGM monomorph actuator.

negligibly small compared with the length l, thus the deflection in thickness and width are neglected; and (2) the cross section of a beam remains plane after deflection and the radius of curvature of a bend beam is large compared with the beam's thickness.

The tensile stress and strain in the FGM monomorph along the x-axis are denoted as T_1 and S_1, respectively, and the electric field along the z-axis in the FGM monomorph is denoted as E_3, the elastic compliance constant is denoted as s_{11}^E ($1/Y$, Y is Young's modulus) and the piezoelectric constant is denoted as d_{31}. The longitudinal strain S_1 at a distance z from the neutral plane d_0 in the direction of x-axis can be expressed as [10]

$$S_1 = -\frac{z - d_0}{\rho} \tag{1}$$

where ρ is the radius of curvature.

Using the constitutive piezoelectric relations, the stress in the ith layer can be expressed as

$$T_{1(i)} = Y_{(i)} S_{1(i)} - Y_{(i)} d_{31(i)} E_{3(i)} \tag{2}$$

The total summation of T_1 over the y–z plane vanishes as the external force vanishes at the free end surface. Thus, the x component of the plane force N_x is

$$N_x = \int_A T_1 \,\mathrm{d}A = w \sum_{i=1}^{n} \int_{((i-1)/h)/n}^{ih/n} \times \left(-\frac{z - d_0}{\rho} Y_{(i)} - Y_{(i)} d_{31(i)} E_{3(i)} \right) \mathrm{d}z = 0 \tag{3}$$

Hence, the position of the neutral plane d_0 can be found to be

$$d_0 = \frac{\rho \sum_{i=1}^{n} Y_{(i)} d_{31(i)} E_{3(i)} + (h/2n) \sum_{i=1}^{n} Y_{(i)} (2i - 1)}{\sum_{i=1}^{n} Y_{(i)}} \tag{4}$$

Since there is no external force or moment exerted on the monomorph, the plane torque vanishes, giving

$$M_x = \int_A T_1 z \,\mathrm{d}A = w \sum_{i=1}^{n} \int_{((i-1)/h)/n}^{ih/n} \times \left(-\frac{z - d_0}{\rho} Y_{(i)} - Y_{(i)} d_{31(i)} E_{3(i)} \right) z \,\mathrm{d}z = 0 \tag{5}$$

Solving Eqs. (4) and (5), the curvature of the monomorph can be obtained as

$$\frac{1}{\rho} = \frac{6 \left[\sum_{i=1}^{n} d_{31(i)} E_{3(i)} Y_{(i)} \sum_{i=1}^{n} (2i - 1) Y_{(i)} - \sum_{i=1}^{n} d_{31(i)} E_{3(i)} Y_{(i)} (2i - 1) \sum_{i=1}^{n} Y_{(i)} \right]}{(4h/n) \sum_{i=1}^{n} (3i^2 - 3i + 1) Y_{(i)} \sum_{i=1}^{n} Y_{(i)} - (3h/n) \left[\sum_{i=1}^{n} (2i - 1) Y_{(i)} \right]^2} \tag{6}$$

In Eq. (6), $E_{3(i)}$ is the electric field in the ith layer. It is dependent on dielectric constant $\varepsilon_{33}^{\mathrm{T}}$ and according to Gauss's law [11], the electric displacements in the adjacent layer (i and $i + 1$) are equal, thus we have

$$\varepsilon_{33(1)}^{\mathrm{T}} E_{3(1)} = \varepsilon_{33(2)}^{\mathrm{T}} E_{3(2)} = \cdots = \varepsilon_{33(i)}^{\mathrm{T}} E_{3(i)} = \cdots = \varepsilon_{33(n)}^{\mathrm{T}} E_{3(n)} \tag{7}$$

If a voltage of V is applied over the cross section, the following relation exists

$$\sum_{1}^{n} E_{3(i)} \frac{h}{n} = V \tag{8}$$

Combining Eqs. (7) and (8), the electric field in the ith layer can be obtained as

$$E_{3(i)} = \frac{nV}{h \varepsilon_{33(i)}^{\mathrm{T}} \sum_{1}^{n} (1/\varepsilon_{33(i)}^{\mathrm{T}})} \tag{9}$$

Following the theory of strength of the materials [12], the displacement δ at the free end of the cantilever beam can be expressed as

$$\delta = \frac{1}{2} \frac{l^2}{\rho} \tag{10}$$

As a result, combining Eqs. (6), (9) and (10), the bending displacement for the FGM monomorph actuator can be obtained.

3. Experimental procedure

The initial powders used for fabricating the monomorph actuator by the EPD technique were two kinds of PZT materials: $Pb(Zr_{0.52}Ti_{0.48})O_3$ (PZT) and $0.95Pb(Zr_{0.52}Ti_{0.48})$

O_3·0.03$BiFeO_3$·0.02$Ba(Cu_{0.5}W_{0.5})O_3$ + 0.5 wt.% MnO_2 (PZT1). The main advantage of this combination is that the two compositions have similar shrinkage during sintering.

The PZT and PZT1 powders were prepared by conventional oxide mixing method. First, the raw oxide powders of PbO (>99.9%), ZrO_2 (>99.9%), TiO_2 (>99.9%), Bi_2O_3 (>99.99%), Fe_2O_3 (>99%), BaO (>99%), CuO (>99.99%), WO_2 (>99%) and MnO_2 (>99.99%) were weighed and mixed with the desired stoichiometrical composition. Considering the volatility of PbO during calcination and sintering, 3% excess of PbO was added into the raw powders. After ball milling for 24 h, the mixed oxides were calcined at 750 and 800 °C for 2 h for PZT1 and PZT, respectively. Then, the calcined powders were smashed and ground by planetary ball milling at the speed of 150 rpm in ethanol for 20 h. Finally, the powders were passed through a 100-mesh sieve to remove the big agglomerations.

Five suspensions for EPD were prepared by adding prepared powders in ethanol with composition as shown in Fig. 1. The suspensions were then subjected to ultrasonic agitation for 10 min. The powder concentration in the suspension was 50 g/l and the suspension pH was controlled to be 4.6 by adding drops of 10% HNO_3 at room temperature. The suspension was stirred for 3–6 h to make sure the complete dissolution and dispersion of the powders in the medium.

The electrophoretic deposition was carried out in an electrophoretic cell, which includes a cathodic conductive foil and a stainless steel counter-electrode. Multilayer deposition technique was adopted. Five suspensions were utilized for deposition consecutively. Each suspension was deposited for five times, with each time last for 1 min. The interval between each deposition was controlled to be 10 min. The time control is important as that the deposit will crack or peel off. The initial applied voltage was 25 V. The voltage was increased by 25 V while changing the suspension since the resistance will increase with the thickness of the deposits. After deposition, the deposits were dried in a dry keeper for 12 h.

The obtained FGM plates were sintered in a furnace at 1100 °C for 1 h. Then they were cut into rectangular-shaped piezoelectric plates and then coated with silver electrode and poled in silicone oil at 100 °C for 2 h under 2 kV/mm. After poling, the fabrication of the FGM piezoelectric monomorph actuator was completed.

The microstructure along the cross section of the FGM actuator was examined using scanning electron microscope (SEM). The displacements were measured using a

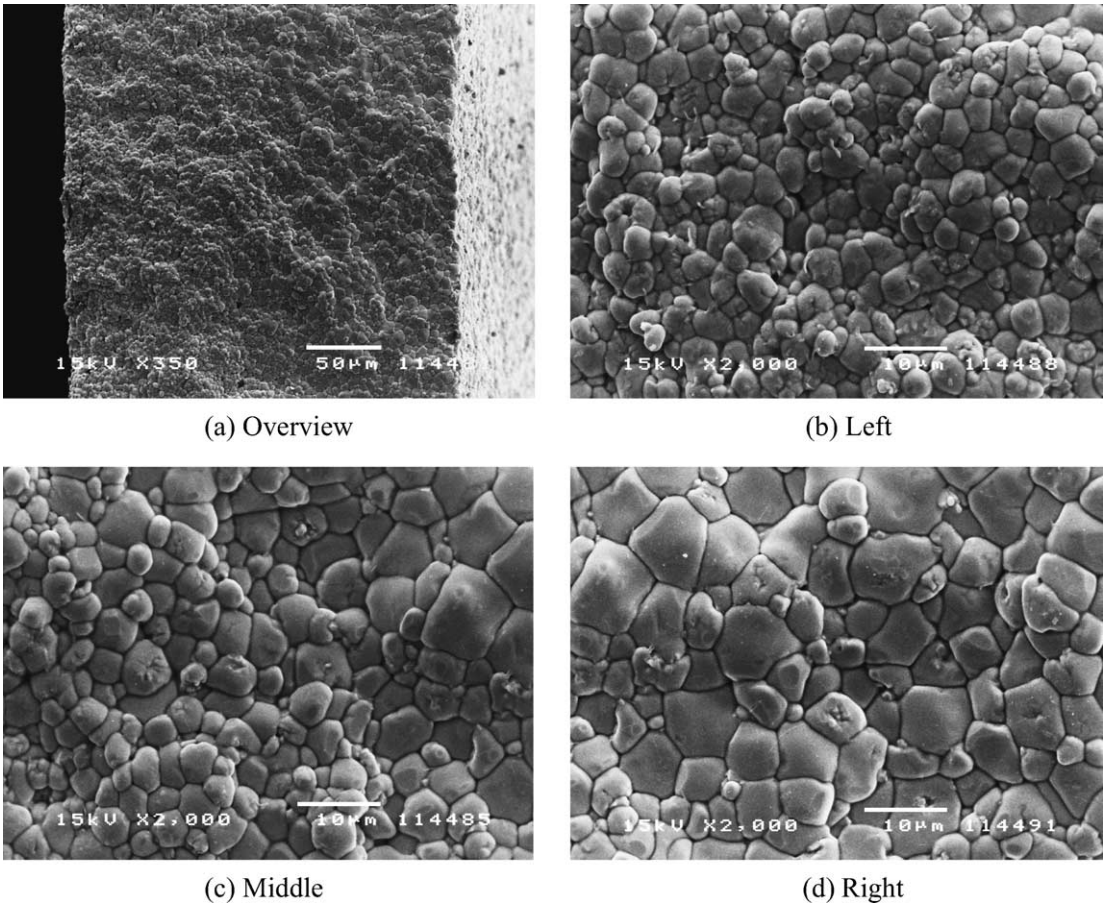

(a) Overview (b) Left

(c) Middle (d) Right

Fig. 2. Gradient variation of microstructure of FGM monomorph along cross section.

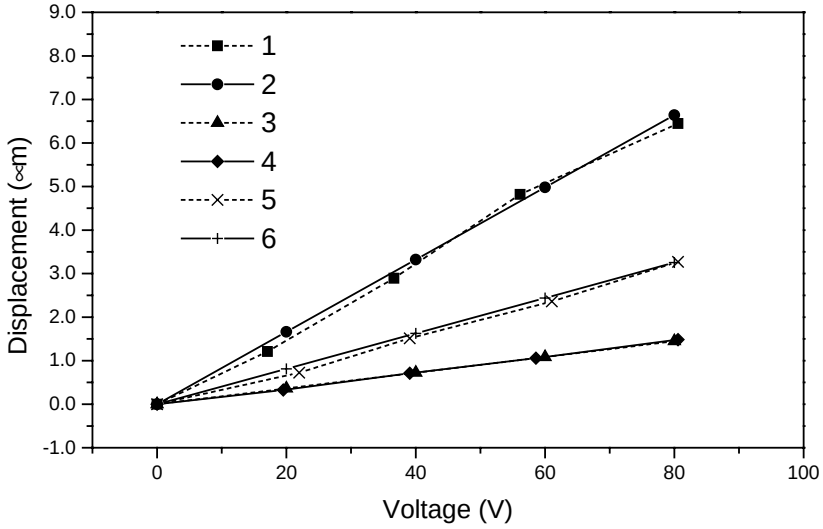

Fig. 3. Comparison of theoretical and experimentally measured displacement as a function of applied voltages of FGM monomorph actuators (lines 1, 3, 5, measured value; lines 2, 4, 6, theoretical value; lines 1 and 2, lines 3 and 4, lines 5 and 6 are for monomorphs A, B and C, respectively).

RT6000HVS ferroelectric tester (Radiant Technologies, Inc.) and an MTI-2000 fotonic sensor (MTI2032RX, MTI Instruments).

4. Results and discussion

Fig. 2 shows the cross section of a FGM plate after sintering at 1100 °C. The cross section has a thickness of approximately 270 μm measured from Fig. 2(a). Over this cross section, the gradient change in microstructure can be observed. From the PZT side (left) to the PZT1 side (right), it can be seen that the grain size gradually increases. This is due to the compositional gradient over the cross section. Fig. 2(b)–(d) shows the left, middle and right side of the cross section with higher magnification, respectively. The variation of piezoelectric properties over the cross section induced by compositional and microstructural gradient is the driving source to actuate the monomorph. The observed image in microstructure gradient also confirms the effectiveness of our procedure to fabricate FGM monomorph actuator.

The bending displacements of three actuators listed in Table 1 with properties in Table 2 were experimentally measured at different voltages and theoretically calculated by combining Eqs. (6), (9) and (10). The results are shown in Fig. 3. It can be found that the bending displacement linearly increases with the applied voltage. The experimentally measured displacements are reasonably close to the theoretical values for all the three actuators. It implies that the derived equations provide good predictions on the bending displacement of a FGM actuator. It is also observed that the thinner and longer actuators give larger displacement. This is because the displacement parabolically increases with the length to thickness ratio (l/h) as seen from Eqs. (6), (9) and (10). Hence, either increasing the length or thinning the thickness can increase the bending displacement. However, thinning of the thickness is more advantageous in device miniaturization because the total dimension can be reduced.

Table 1
Dimensions of the FGM monomorphs for displacement measurement

Monomorph	Width, w (mm)	Thickness, h (mm)	Length, l (mm)
A	3.40	0.14	10.00
B	2.91	0.30	10.00
C	3.00	0.30	15.00

Table 2
Piezoelectric properties of the materials applied in each layer

Properties	1	2	3	4	5
Y ($\times 10^{10}$ Pa)	7.49	6.94	7.21	7.21	7.91
d_{31} ($\times 10^{-10}$ m/V)	−0.84	−0.77	−0.90	−0.79	−0.30
ε_{33}^{T} ($\times 10^{-8}$ F/m)	1.05	1.10	1.09	0.94	0.76

5. Conclusions

A FGM monomorph fabricated by the EPD technique is introduced in this paper. It utilizes a built-in functional gradient that is obtained by aligning gradient compositions along the thickness of the monomorph actuator. After sintering, the gradient change in microstructure was observed over the cross section. The expression for the bending displacement of the actuator was derived, which relates the bending displacement to the geometrical properties (l, w, h and n), material properties (Y, d_{31} and ε_{33}^{T}) and the applied voltage V. The experimental results have shown good consistency with the theoretical predictions.

References

[1] K. Uchino, Ceramics actuators: principles and applications, MRS Bull. 18 (1993) 42–48.
[2] J.G. Smits, S.I. Dalke, T.K. Cooney, The constituent equations of piezoelectric bimorphs, Sens. Actuators 28 (1991) 41–46.
[3] X.H. Zhu, Z.Y. Meng, Operational principle, fabrication and displacement characteristics of a functional gradient piezoelectric ceramic actuator, Sens. Actuators 48 (1995) 169–176.
[4] C.C.M. Wu, M. Kahn, W. Moy, Piezoelectric ceramics with functional gradients: a new application in material design, J. Am. Ceram. Soc. 79 (1996) 809–812.
[5] W.F. Shelley II, S. Wan, K.J. Bowman, Functionally graded piezoelectric ceramics, Mater. Sci. Forum 308/311 (1999) 515–520.
[6] A. Almajid, M. Taya, S. Hudnut, Analysis of out-of-plane displacement and stress field in a piezocomposite plate with functionally graded microstructure, Int. J. Solids Struct. 38 (2001) 3377–3391.
[7] M. Nagai, Y. Yamashita, Y. Takuma, Electrophoretic deposition of ferroelectric barium titanate thick films and their dielectric properties, J. Am. Ceram. Soc. 76 (1993) 153–255.
[8] B. Ferrari, R. Moreno, Electrophoretic deposition of aqueous alumina slips, J. Eur. Ceram. Soc. 17 (1997) 549–556.
[9] P. Sarkar, X. Huang, P.S. Nicholson, Structure of ceramic microlaminates by electrophoretic deposition, J. Am. Ceram. Soc. 75 (1992) 2907–2909.
[10] M. Marutake, M. Yokosuka, Electromechanical properties of composite bending-type transducers, Jpn. J. Appl. Phys. 34 (1995) 5284–5287.
[11] S.Z. Cheng, Z.Y. Jiang, Physics, Advanced Education Press, China, 1979.
[12] W.A. Nashi, Strength of Materials, McGraw-Hill, Inc., 1994.